We are IntechOpen, the world's leading publisher of Open Access books Built by scientists, for scientists

6,900
Open access books available

185,000
International authors and editors

200M
Downloads

Our authors are among the

154
Countries delivered to

TOP 1%
most cited scientists

12.2%
Contributors from top 500 universities

WEB OF SCIENCE™

Selection of our books indexed in the Book Citation Index in Web of Science™ Core Collection (BKCI)

Interested in publishing with us?
Contact book.department@intechopen.com

Numbers displayed above are based on latest data collected.
For more information visit www.intechopen.com

16

Land-Cover Classification Using Self-Organizing Maps Clustered with Spectral and Spatial Information

M. L. Gonçalves[1], J. A. F. Costa[2] and M. L. A. Netto[3]
[1]*Department of Computer Science,*
Pontifical Catholic University of Minas Gerais, Poços de Caldas, MG
[2]*Department of Electrical Engineering*
Federal University of Rio Grande do Norte, Natal, RN
[3]*School of Electrical and Computer Engineering*
State University of Campinas, Campinas, SP
Brazil

1. Introduction

Digital classification methods of remotely sensed images have acquired a growing importance in the automatic recognition of the land cover patterns. The enormous quantity of images that are being generated from an increasing number of highly sophisticated sensor systems require the development of innovative classification methodologies, which allow an automatic and efficient detection of the great volume of data available in the images and at the same time makes the mapping process of terrestrial surfaces less subjective and with greater potential for reuse in subsequent situations.

Particularly, unsupervised classification methods have traditionally been considered as an important approach for the interpretation of remotely sensed images. This approach of classification plays an especially significant role when very little a priori information about image data is available, and for that reason continues to be a popular choice for analysts without ample field knowledge or for those wanting to avoid introduced bias in classification analysis (Duda & Canty, 2002; Kelly et al., 2004).

Unsupervised classification is frequently performed through clustering methods. These methods examine the unknown pixels in an image and incorporate them into a set of classes defined through the natural clusters of the gray levels of the pixels. Cluster analysis provides a practical method for organizing a large set of data so that the retrieval of information may be made more efficiently. However, although there is a large quantity of different clustering methods in the pattern recognition area (Xu & Wunsch II, 2005), only a limited quantity of them can be used in remote sensing applications. As pointed out in Tran et. al. (2005), several problems are encountered when clustering remotely sensed images, but above all the image size and the feature dimension problems are those that often make a method inappropriate due to computation time and computer memory.

The most common clustering method applied to remotely sensed data is partitional. The majority of software or computational systems meant for the digital processing of remotely

sensed images specifically contain two partitional clustering algorithms to perform unsupervised classification: the K-means algorithm, and a variation of it, the ISODATA (Ball & Hall, 1967). Despite being widely used, these partitional clustering methods have various limitations. The objective functions that they use begin with the assumption that the number of classes, K, is known a priori. In the hypothesis that an inadequate K' value has been chosen, the method will impose, through the use of optimization techniques, K' clusters to the data. The user must also manually specify various parameters in order to control the clustering process, among them: the initial centroids of each cluster, the maximum number of iterations, thresholds to perform the division, fusion, or exclusion of clusters. K-means and ISODATA are very sensitive to these parameters, which can generate different partitions when various simulations are done for the same data set. Facing this, the optimal value of these parameters is frequently encountered through trial and error. These needs certainly increase the level of interaction between the user and the computational algorithm, consequently increasing the degree of subjectivity of the categorization process of the image. Other no less important limitations of partitional algorithms, such as K-means and ISODATA, are: the high computational cost when the data to be analyzed is very large (at each iteration, all of the pixels in the image are compared with all of the clusters centroids) and the existence of suppositions about the cluster forms. Generally only one prototype (centroid) is used to represent a cluster, thus these methods become adequate only for the analysis of clusters that have hyper-spherical formats (Shah et al., 2004).

Another possible, though uncommon, way of performing unsupervised classification of remotely sensed images is through hierarchical clustering methods. Unlike partitional methods, hierarchical methods do not require the user to specify the number of clusters and other additional parameters beforehand, and therefore are not affected by initialization and local minima. Another significant advantage of these methods is that they make it possible to visualize the result of the classification by means of a dendrogram which illustrates in a hierarchical form the degree of similarity between the clusters that are formed by fusions (or divisions) at each successive stage of the analysis. However, hierarchical methods have some characteristics that prevent their application in the classification of remotely sensed images: (a) in general they require memory space in the order of $O(N^2)$, in which N is the number of records in the data set; (b) dendrograms are impractical for large data sets, and therefore the results can be difficult to interpret; (c) in order to determine the cut-off of the dendrogram (ideal number of clusters) some decision criteria must be applied (Duda & Canty, 2002; Kelly et al., 2004).

Consequently, hierarchical clustering modules are rare in remote sensing software packages and for this reason are normally utilized in an uncoupled way. In the literature, there is not much research that makes use of hierarchic methods in unsupervised classification of remotely sensed images, and in general common versions of these methods are applied in practice when the main objective is basically to compare performance with other unsupervised methods (Duda & Canty, 2002; Wilson, et al., 2002). However, a relatively recent progression of approaches attempting to make the use of hierarchical clustering methods viable in remote sensing applications can be seen. For instance, instead of applying agglomerative hierarchical methods directly on a pixel by pixel basis, some works have employed these methods only after the application of some other clustering method on the original image data. In Tran et al. (2003) the K-means algorithm was used to classify the image data before the application of a hierarchical method, and the ISODATA was used for the same reason in Marçal & Castro (2005) and in Marçal & Borges (2005). Although this

strategy is effective at preventing the (expensive) application of hierarchic methods to large data sets, a possible disadvantage of it is that the results of the classification methods presented in these works can be influenced by the limitations of the K-means and ISODATA algorithms, which were mentioned earlier here.

Evidently, the literature contains other proposals for unsupervised methods to classify remote sensing data that do not make use only of conventional clustering approaches (Huang, 2002; Shah et al., 2004; Tso & Olsen, 2005). In a special way, a number of researchers have proposed several sophisticated approaches to classify remote sensing images based on computational intelligence methods like neural networks, fuzzy systems, and evolutionary algorithms (Bandyopadhyay, 2005; Ji, 2003; Liu et al., 2005).

Particularly, some works has investigated the use of the Kohonen neural network (more commonly known as SOM - Self-Organizing Map) for the task of clustering and classification of remotely sensed images. Ji (2000) showed that the SOM algorithm is capable of achieving higher classification accuracy as compared to that of the maximum-likelihood method and concluded that the neural network is a useful viable alternative for the classification of remotely sensed images. Vilmann et al. (2003) studied the effect of the application of several extensions of the SOM in the cluster analysis of multispectral and hyperspectral images. The authors showed excellent data clustering and classification, and concluded that some considerations about the consequence of the dimensionality reduction produced by SOM must still be investigated. In Hadjimitsis (2003), an unsupervised classification method using SOM was proposed for mapping land-cover changes. Preliminary results show that utilizing SOM for image classification is efficient and opens up significant area for further research.

Although SOM has been considered as an effective tool for clustering in remote sensing images, it is worth noting that the detection of cluster boundaries through the output space of the network is not a trivial task. Moreover, as described in Ji (2000) the process of segmentation of the trained neural map can affect representation of the classes. Consequently, the majority of the classification methods based on SOM carry out the cluster detection with the help of an image analyst that manually segments the neural map using a priori knowledge of the data and some alternative tool to make cluster visualization easier in SOM (Merkl & Rauber, 1997). In this way, the analyst interacts with the cluster analysis process by visualizing and interpreting the trained map. However, in unsupervised classification approaches that have as basic objective to discover the inherent structure of the data, the detection of clusters through SOM neurons must be done without user interference.

Faced with this scenario, this work presents a methodology for unsupervised classification of remotely sensed images that employs a two-level clustering approach, where the image data are first clustered using the SOM, and then the SOM is automatically segmented without any user intervention. This strategy considerably reduces the computational complexity of the data analysis and provides significant advantages over conventional unsupervised classification techniques, such as K-means and ISODATA. In this purpose, the prototype vectors of the SOM, which represent the original patterns of the image, are clustered through an agglomerative hierarchical clustering method generating a simplified dendrogram for the image data. The SOM neighborhood relation is used to constrain the possible merges in the construction of the dendrogram. In addition, spatial information measures and a cluster validation index calculated in a modified manner using the vector quantization property of the SOM are incorporated into merging criterion of neighboring clusters. The experimental results show examples of the application of the proposed classification methodology and compare its performance with the K-means algorithm.

2. The SOM

The SOM is certainly one of the main models of neural networks at present and is used in countless applications. Unlike other neural network approaches, the SOM is a type of neural net based on competitive and unsupervised learning (Kohonen, 1997). The network essentially consists of two layers: an input layer *I* and an output layer *U* with neurons generally organized in a 2-dimensional topological array. The input to the net corresponds to a *p*-dimensional vector, $\boldsymbol{x}$, generally in the space $\Re^p$. All of the *p* components of the input vector feed each of the neurons on the map. Each neuron *i* can be represented by a synaptic weight vector $\boldsymbol{w_i} = [w_{i1}, w_{i2},..., w_{ip}]^T$, also in the *p*-dimensional space. For each input pattern $\boldsymbol{x}$ a winner neuron, *c*, is chosen, using the criterion of greatest similarity:

$$\left\| x - w_c \right\| = \min_i \left\{ \left\| x - w_i \right\| \right\} \tag{1}$$

where $\|.\|$ represents the Euclidian distance. The winner neuron weights, together with the weights of the neighboring neurons, are adjusted according to the following equation:

$$w_i(t+1) = w_i(t) + h_{ci}(t)\left[x(t) - w_i(t)\right] \tag{2}$$

where *t* indicates the iteration of the training process, $\boldsymbol{x(t)}$ is the input pattern and $h_{ci}(t)$ is the nucleus of neighborhood around the winner neuron *c*.

Once the SOM training algorithm has converged the computed feature map displays important statistical characteristics of the input space, which can be summarized as follows:

i. Vector quantization: the basic objective of SOM is to store a large set of input vectors by finding a smaller set of prototypes that provides a good approximation to the input space.
ii. Topological ordering: the features map computed by SOM is ordered topologically. Similar input vectors are mapped close to each other, while dissimilar ones are mapped far apart.
iii. Density Matching: the SOM reflects the probability distribution of data in the input space. Regions in the input space in which the input patterns are taken with a high probability of occurrence are mapped onto larger domains of the output space, and thus have better resolution than regions in the output space from which input patterns are taken with a low probability of occurrence.

3. The proposed method

The methodology proposed in this work attempts to exploit the characteristics and properties of the SOM to perform the unsupervised classification of remotely sensed images. The key point of the proposed method is to perform the cluster analysis of the image through a set of SOM prototypes instead of working directly with the original patterns of the scene. For this, the classification task is carried out using a two-level SOM-based clustering approach.

The two clustering levels, which consist basically of the training and segmentation of the SOM, are illustrated in Fig. 1 and described in greater detail in the next subsections.

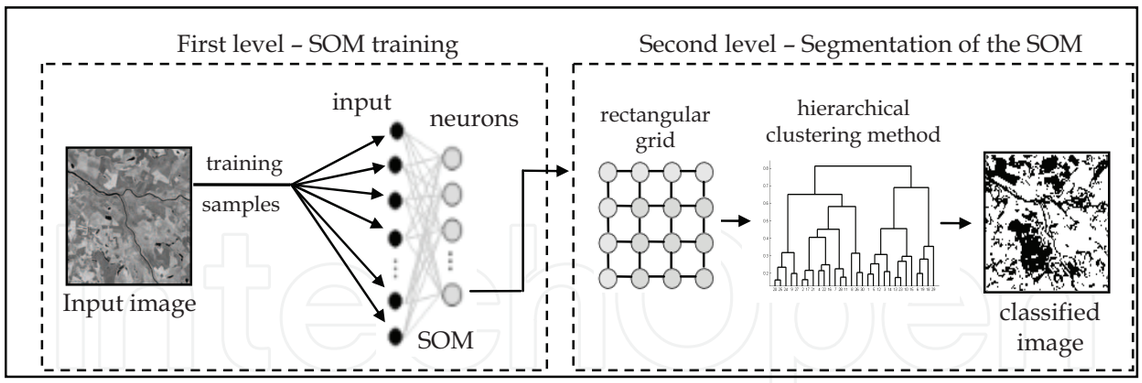

Fig. 1. Illustration of the proposed classification methodology

3.1 First level clustering – SOM training

At the first clustering level the SOM is used to map the original patterns of the image to a reduced set of prototypes arranged in a two-dimensional rectangular grid. The objective is to quantize and to represent the image patterns in a space of smaller dimension, seeking to preserve the probability distribution and topology of the input space. In this processing level, two important factors should be considered: the sampling process of the input image and the determination of the SOM training parameters.

3.1.1 Image sampling process

Unlike pixel by pixel approaches that only use the spectral information of individual points to find homogenous regions; the proposed method performs the sampling of the image through pixel windows. The idea is to incorporate in the classification process information about the neighborhood (context) of the pixels, considering that isolated pixels are not able to represent the majority of cover land patterns, especially in the case of images that have higher spatial resolutions. Even though the strategy of using information from neighboring pixels has a greater computational cost that the pixel by pixel approach, in the literature various works have shown that this effort is justified by a proportional increase in classification accuracy (Magnussen et al., 2004).

In this purpose, the sample windows are collected uniformly across the entire region of the image, without overlappings and at regular intervals. All of the samples are square and have the same size. The determination of the size of samples is not a process that can be easily automated. Depending on the characteristics of the image to be classified, windows that are too small might not capture the particular pattern of the land cover classes, while larger windows might include pixels from more than one class. Nevertheless, beginning with a size no smaller than 3×3, the user has within the proposed methodology a certain degree of flexibility to define the dimensions of the sample windows, and this is not therefore a critical point in the process. The proposed method (in the second level clustering) processes in a special way the SOM prototypes that represent sample windows which incorporate more than one class (heterogeneous prototypes).

3.1.2 SOM parameters

When the SOM is used some parameters must be specified to define the structure of the map and to control its training process. Based on the existing literature, on experimental tests,

and some peculiarities of the application of SOM on remotely sensed images, the proposed classification methodology utilizes the following parameters and criteria to train the SOM:

a. Linear initialization of weights: Although the random initialization is the most common form to initialize SOM weights, Kohonen defends the idea of linear initialization, since this permits the learning algorithm to directly enter the convergence phase, as well as avoiding undesirable skews in the array (Kohonen, 1997).
b. Batch training mode: The batch training mode makes the result of the SOM mapping insensitive to the presentation order of the input patterns. This can be done by adding the average of the contributions of all of the input patterns for each neuron. This average displacement has been leading to better results than the conventional SOM algorithm in which the neurons are updated every time a new input pattern is provided to the net.
c. Gaussian neighborhood function: Instead of utilizing the "bubble" type neighborhood proposed in the original SOM algorithm, the Gaussian type neighborhood is employed in the proposed method because it better emphasizes the clusters in terms of distances between neurons (Kohonen, 1997).
d. Rectangular array: The rectangular shape was chosen to organize the array of the neurons of the net, not just because it is the most commonly used, but also because it is the best at generating an image of the SOM features map, which will be described ahead.
e. Stopping criteria: To determine the number of training epochs the disorder measure "AUD" (Average Unit Disorder) proposed by Azcarraga (2000) was used in this approach. Essentially, AUD evaluates the degree of organization of the SOM during the training process through the differences of synaptic weights and geometric distance between neurons in the rectangular grid. The SOM is considered sufficiently trained when the AUD measure does not change in value by more than a certain threshold.
f. Size of the map: The dimension of the map is one of the free parameters of SOM that particularly depends on the input image and the objectives of the classification. If the objective is to detect all of the patterns in the image, including those with low probability of occurrence, large-sized maps must be employed in the analysis; in the opposite case, if the interest is concentrated only on the predominant patterns in the scene, a smaller-sized SOM can be utilized. Nevertheless, the performance of the proposed classification methodology is not significantly affected if sufficiently large sizes for the SOM are utilized. While maps with larger dimensions than are necessary have a larger quantity of inactive neurons, this event is not prejudicial within the proposed methodology. Just as the method deals with the heterogeneous prototypes in an adequate manner, the same occurs with inactive prototypes.

3.2 Second level clustering – segmentation of the SOM

Unlike in other applications in which the SOM is used as a visual aid tool to indicate cluster tendencies, in this work the detection of clusters through trained SOM is executed without user intervention. Thus, after completion of training performed by the SOM, the second level of the proposed methodology basically consists of segmenting the SOM output map using an additional clustering method.

Several approaches have been proposed for clustering the neurons of a trained SOM (Costa & Netto, 1999; Costa & Netto, 2001; Gonçalves et al., 2005; Gonçalves et al., 2006). Approaches that make use of conventional cluster methods, such as K-means and

hierarchical clustering, are those most commonly applied (Sezgin et al., 2004; Vesanto & Alhoniemi, 2000; Wang, 2002). However, it is worth noting that methods based on K-means algorithm are only feasible for hyper-spherical-shaped clusters and approaches based on classical hierarchical clustering only use inter-cluster distance information to merge the nearest neighboring clusters. Seeking to overcome the limitations of these approaches, Wu & Chow (2004) proposed then a hierarchical algorithm for clustering the SOM that uses more information about the data in each cluster in addition to inter-cluster distances. To determine which pair of clusters to be merged the proposed algorithm locally uses the CDbw clustering validity index (Composing Density Between and Within Clusters), presented in Halkidi & Vazirgiannis (2002), which allows to incorporate the inter-cluster and intra-cluster density into merging criteria in addition to distance information. Wu and Chow showed that the algorithm proposed by them clusters data better than the classical clustering algorithms on the SOM.

For this reason, the classification methodology proposed in this work employs a hierarchical method for clustering the SOM that also uses the CDbw clustering validity index to decide which pair of clusters to be merged. However, instead of using the original data to perform the calculation of the CDbw index (as is made in Wu & Chow (2004)), the algorithm applied here executes the computation of the CDbw index using the own prototype vectors of the trained SOM (which represent the image original data). Furthermore, the adopted merging criterion also incorporates two spatial information measures and still uses neighborhood relation between the neurons in the SOM grid to constrain the possible merges.

3.2.1 Prototypes filtering

Seeking to guarantee even greater efficiency in the segmentation process of the trained SOM, before the hierarchical clustering algorithm is applied, the proposed method filters two types of prototypes that generally appear in the mapping of image patterns through SOM. These prototypes are called inactive and heterogeneous.

The inactive prototypes correspond to the neurons that have null activity in the SOM competitive learning process, i.e., they are not associated with any input patterns. These prototypes are simply discarded of the analysis.

Heterogeneous prototypes are those that have a high degree of spectral-textural heterogeneity and are normally associated with input patterns that incorporate more than one land cover class. Most of the time, these patterns correspond to transition regions between land cover classes present in the image and are captured in consequence of the sampling through pixel windows. The heterogeneous prototypes are not considered by the hierarchical clustering method applied to segment the SOM. The objective of excluding these prototypes is to prevent them (and consequently the input patterns associated with them) from being erroneously attributed to one of the classes that are part of them. Heterogeneous prototypes can be seen as noisy or divergent patterns, and if they are not filtered the hierarchical method can incorporate them in the clusters that will be produced or retain them in separate clusters. Because of this, the input patterns associated with these heterogeneous prototypes are classified only at the end of the analysis, considering the neighboring pixels that have already been labelled.

In the proposed classification methodology the spectral-textural heterogeneity degree of each SOM prototype is computed from Haralick's co-occurrence matrix (Haralick et al., 1973). Since the weight vectors of the SOM prototypes have the same dimensions as the input patterns (that in this case are pixel windows), it makes it possible to generate an image

of each prototype of the net and to calculate the co-occurrence probability of all pairwise combinations of grey levels in each one of them. The energy (sometimes called uniformity) was the measure chosen to calculate the spectral-textural heterogeneity of each prototype from co-occurrence matrix. This measure, described through the equation (3), gets values next to 1 when the area of interest presents uniform texture (similar grey levels), and values that tend to zero when the area is not uniform.

$$ENE = \sum_i \sum_j P(i,j)_{d,\theta} \tag{3}$$

where $P(i,j)_{d,\theta}$ is the co-occurrence probability of two grey levels i and j, separate to a distance d in the direction θ. The prototypes whose *ENE*'s satisfy the relationship given below are considered heterogeneous and are consequently filtered:

$$ENE < \mu_{ENE} - \frac{1}{2}\sigma_{ENE}. \tag{4}$$

Here μ_{ENE} and σ_{ENE} are, respectively the average and the standard deviation of the *ENE*'s of all of the SOM prototypes.

The processing time consumed by this filtering step is compensated not just by the reduction of the number of SOM prototypes that will be analyzed by the hierarchical clustering method, but mainly by a possible increase in the precision of the image classification. In addition, inactive and heterogeneous prototypes can act as "interpolation units" or "borders" in the SOM grid, facilitating the separation of the clusters.

3.2.2 Hierarchical clustering method

If an agglomerative hierarchical clustering method is applied to the SOM neurons it must respect the topological relationships of the neural net output space. Unlike traditional hierarchical clustering methods, which consist of comparing all of the pairs of objects to decide on a fusion, the approach utilized in this work verifies the possibility of fusions only between adjacent neuron pairs in the SOM grid. As shown in Fig. 2, given a $m \times n$ neurons grid, the neuron in position (3,2), for example, only has possibility of fusion with neighboring neurons in positions (2,1), (2,2), (2,3), (3,1), (3,3), (4,1), (4,2) and (4,3). This approach significantly diminishes the processing cost of the hierarchical clustering method applied.

Other important characteristic of the hierarchical method utilized for clustering the SOM is in its merging criterion. It utilizes more information about the pair of clusters than traditional methods. As mentioned earlier, the CDbw clustering validity index which allows to incorporate inter-cluster and intra-cluster density information is used in conjunction with two spatial information measures to determine which cluster pair to be merged.

Although the CDbw index has a reasonable computational complexity in comparison with others clustering validity indexes (Halkidi & Vazirgiannis, 2002), the local use of it to decide about the cluster fusion added to the large data volume that normally arises from remote sensing images may require a considerable processing time for clustering the SOM. For this reason, seeking to reduce the processing volume, instead of calculating the CDbw index directly on image original data the method proposed here performs the calculation of it using the own SOM prototype vectors (which represent the image original data).

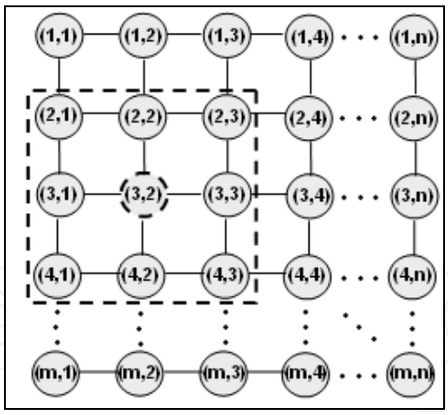

Fig. 2. Adjacent neurons in the SOM grid

Even though the SOM performs a good approximation of the input space, it is true that the strategy of applying a validation index on the network prototypes instead of applying them directly to the original pattern can cause some numerical difference in the results. To diminish possible approximation errors, the proposed method modifies the way that CDbw index is calculated. The index is calculated by utilizing not just the weight vectors of the SOM prototypes, but also the activity level of each one of them. The activity level of one prototype is equal to the number of input patterns that are associated to it by the SOM mapping process.

An example of the modifications applied to the calculation of CDbw index can be described through the equation (5). This formula represents the calculation of the standard deviation vector (σ) of a data cluster *C*:

$$\sigma = \sqrt{\frac{1}{n}\sum_{i=1}^{n}\left(x_i - \mu\right)^2} \tag{5}$$

where x_i is the data belonging to the cluster *C*, *n* is the number of data points in *C*, and μ represents the sample mean of the same cluster.

Applying the strategy of modifying the index calculation, the computation of the standard deviation vector of a data cluster *C*, equivalent to equation (5), becomes formulated in the following way:

$$\sigma^{som} = \sqrt{\frac{1}{n}\sum_{i=1}^{m} h(w_i).\left(w_i - \mu^{som}\right)^2} \tag{6}$$

in which wi is the SOM prototype, h(wi) is the activity level of prototype wi, m is the number of SOM prototypes that represent data from cluster C, n is the number of data points in C, and μsom represents the sample mean of the cluster C, which is computed as follows:

$$\mu^{som} = \frac{1}{n}\sum_{i=1}^{m} h(w_i).w_i \tag{7}$$

Whereas the calculations of σ and μ use all of the points belonging to *C*, σ^{som} and μ^{som} only uses the SOM prototypes. Therefore it can be observed that σ^{som} is an approximate

calculation of σ, but with a lower processing cost, since the number of data points n is generally much smaller than number of SOM protoypes m. The inclusion of the activity levels $h(.)$ of the prototypes in the calculation of σ^{som} helps to reduce the effect of quantization error caused by SOM mapping.

The strategy of using SOM prototypes and its activity levels instead of the original data is applied to all the steps of the CDbw index algorithm. This modified version of the CDbw index is therefore locally applied to each neighboring cluster pair at all of the levels of the dendrogram produced by hierarchical method used for clustering the SOM. The pair of clusters with the lower value of the CDbw is considered that one with the strongest tendency to be clustered. The values of the CDbw index for all clusters pairs (i,j) (designated as $CDbw_{ij}$) are normalized within the interval [0,1].

The spatial information incorporated in the merging criterion is calculated through two indices, denominated *spatial boundary index* and *spatial compactness index*. These indices, projected by Marçal & Castro (2005), are computed here from classified image using the SOM prototype clusters in each level of the dendrogram generated by hierarchic method.

The spatial boundary index (B_{ij}) calculates the boundary length between all class pairs (i,j) considering eight neighbors for each pixel (four adjacent and four oblique). Its formula is given as follows:

$$B_{ij} = 1 - \frac{1}{2}\left(\frac{b_{ij}}{\sum_{k=1(k\neq i)}^{N} b_{ik}} + \frac{b_{ij}}{\sum_{k=1(k\neq j)}^{N} b_{kj}} \right) \tag{8}$$

where b_{ij} is the number of boundary counts for the class pair (i,j) and N is the number of classes (SOM prototypes) in the dendrogram level that is being analyzed. This index provides values within the interval [0,1], with lower values when the boundary between the pair of classes is considerable. According to idea behind this index, two classes with an extensive common boundary must be more inclined to merge than classes with very little or no common boundaries (Marçal & Castro, 2005).

The spatial compactness index (C_{ij}), defined through the equation (9), is based on the number of self-boundary counts (b_{ii}) for each class. This index penalizes the merger of compact classes. The index C_{ij} also results values between 0 and 1, with lower values when the class is composed of isolated pixels.

$$C_{ij} = \frac{1}{2}\left(\frac{b_{ii}}{b_{ii} + 6\sum_{k=1(k\neq i)}^{N} b_{ik}} + \frac{b_{jj}}{b_{jj} + 6\sum_{k=1(k\neq j)}^{N} b_{jk}} \right) \tag{9}$$

The merging criterion adopted here for clustering the SOM establishes that the pair of prototype classes (i,j) with the lowest value resultant of the average computed between $CDbw_{ij}$, B_{ij} and C_{ij} must be selected for merger.

At the end of this processing level there is a dendrogram that shows in a hierarchical way the similarity levels between the SOM prototypes. Remembering that the SOM prototypes

represent all of the input patterns; the obtained dendrogram reflects the relationships that exist between the original image data, and it can be considered therefore as a simplified dendrogram of the image.

3.2.3 Image classification

At each level of the dendrogram produced by the hierarchical method there is a different cluster configuration for the SOM prototypes that can be utilized to represent the classes by which the original image will be classified. Thus, as with any hierarchical clustering method, some decision criterion needs to be applied in order to verify which level of the dendrogram represents the ideal cluster configuration (or the ideal number of classes).

According to Vesanto & Alhoniemi (2000), the most typical solution is to cut the dendrogram where there is a large distance between two merged clusters. However, this approach ignores the fact that the within-cluster distance may be different for different clusters. Therefore, the decision criterion used here consists of applying once more the CDbw index (in its modified version) as a function of the number of clusters at all levels of the dendrogram, and choosing the level at which the index presents its optimum value among the values obtained.

Having defined the dendrogram level that presents the best cluster configuration for the SOM prototypes, and consequently for the image patterns, the SOM is then labeled. According to the proposed methodology, each discovered land cover class will be therefore represented by a group of SOM prototypes and not just one single prototype as occurs in the majority of the partitional clustering methods, such as *K*-means algorithm.

In order to classify the image, pixel windows are collected from the original image with equal dimensions from the training sample and are compared to all of the SOM prototypes (including also the heterogeneous prototypes). This comparison is performed through the distances calculated between the pixel windows and each of the prototypes. The central pixel of the pixel window receives the label of the prototype that has the least distance from it. The image is then entirely run through until all of the pixels have been classified.

In the end, the results of the classification process performed are improved. The pixels in the image that receive the label of the heterogeneous prototypes class are reclassified. Each one of these pixels is compared to its neighboring pixels in the image that have not been labeled by the heterogeneous prototype class, and it receives a new label that will be the same as the neighbor that has the smallest distance from it in terms of spectral features.

4. Experimental results

This section shows examples of the application of the proposed classification methodology on two test images. The results are compared with those obtained by applying the K-means algorithm to the same images. It is worth emphasizing that the comparisons performed here refer to the results obtained by two algorithms with significantly different principles and characteristics and therefore this work do not intend to decide which method is better, but to analyze the applicability and the benefits of the proposed classification methodology.

4.1 Experiment 1

This experiment was performed on a segment taken from a CBERS image (provided by National Institute for Space Research, INPE, Brazil). It has an IFOV of 20 m and is composed of three bands in the visible spectrum. This imagery was acquired on 4 August 2005 and

shows part of the city of Rio de Janeiro, Brazil. The scene (392×394 pixels) presents four large land cover classes: urban area, vegetation, sandy soil and water. Fig. 3 shows a color composite of the segment of the original image (denominated here as test image 1).
Application of the proposed methodology was initially performed with a sampling process of the scene. Sample windows of size 7×7 were collected uniformly across the entire region of the image, without overlapping and at regular 10 pixel intervals, resulting in a total of 1521 samples obtained without user intervention.

Fig. 3. Color composite of the test image 1

A SOM composed of 64 neurons arranged in a 8×8 rectangular grid was trained with all of the samples previously collected. As mentioned earlier, the weight vectors of each neuron have the same dimensions as the input patterns (that in this case are pixel windows of size 7×7), it makes it possible to generate an image of each SOM prototype. Fig. 4a shows the images of each SOM prototype arranged in the rectangular grid after the training. By means of them it is possible to visualize the properties of the mapping produced by the neural net. The four land cover classes present in the original image appear in the form of clusters on the SOM grid image. In the upper right corner the prototypes associated with the water pattern are found, in the upper left corner the prototypes associated with the vegetation pattern are present, in the lower right those that correspond to urban area are found, and in the lower left corner there are prototypes associated with sandy soil class. If we observe the original image, we can verify that the sandy soil class occupies the least area in the scene. Because of this, since the SOM reflects the probability distribution of the input data, the prototypes associated with sandy soil class (in nearly white tones on the SOM grid image) are present in a lesser number than the other prototype classes. SOM's topological ordering property can also be seen. The prototypes of the water and sandy soil classes are isolated to one another in the SOM grid, because the input patterns (samples) corresponding to these two classes are the least spectrally similar in comparison with the spectral attributes of the other two land cover classes. While the SOM grid image is useful for visualizing the SOM mapping, it must be pointed out that in the method proposed here no interaction by the user is done on it.
After the SOM training, the prototype filtering process was applied. In this experiment, 4 SOM prototypes presented null activity, and 8 presented a high degree of spectral-textural heterogeneity, given that its *ENE* values exceeded the threshold defined in the equation (4). Thus, of the 64 total SOM prototypes, 12 of them were filtered, leaving 52 to be analyzed.

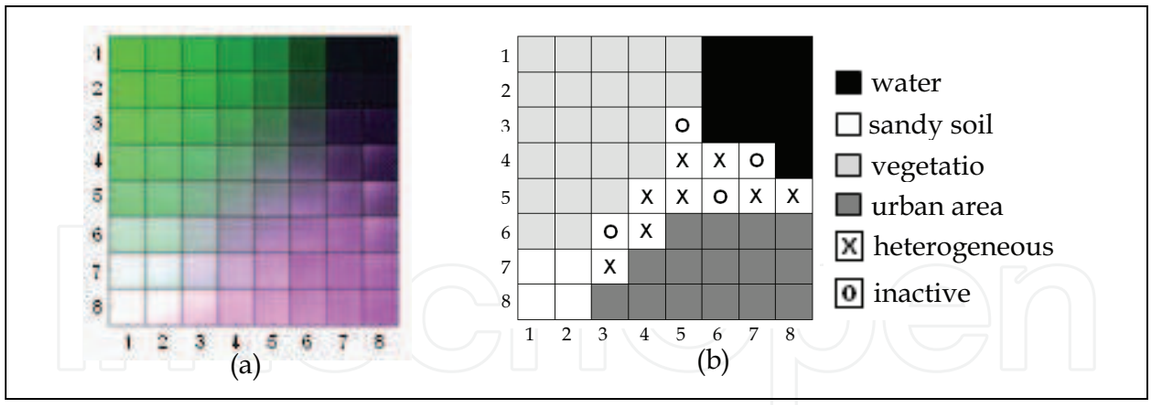

Fig. 4. (a) SOM grid image obtained from test image 1. (b) Classified SOM grid.

In sequence, the agglomerative hierarchical method was applied on the filtered SOM prototypes. Consequently, a dendrogram consisting of 52 levels was generated, each level with a different configuration of SOM prototype clusters. Fig. 5a shows the dendrogram obtained using the merging criterion employed by the proposed method. As can be viewed with the aid of the SOM grid image (Fig. 4a), the SOM prototypes corresponding to four land cover classes present in the image were appropriately clustered in a hierarchical way at all of the stages. Attempting to confirm the efficiency of the implemented merging criterion, the single linkage method also was utilized for clustering the SOM prototypes, but using only the spectral information of the SOM prototypes and respecting its topological relations in the grid. The single linkage method is the most popular method of hierarchical clustering. Single linkage defines the distance between any two clusters as the minimum distance between them (Xu & Wunsch II, 2005). The Fig. 5b shows the dendrogram produced by the single linkage method. For the test image 1 this is not a satisfactory result. The SOM prototypes corresponding to sandy soil class (located in the positions (7,1), (7,2), (8,1), and (8,2) of the SOM grid) were all merged with SOM prototypes corresponding to area urban class at the earliest levels. This occurs because the prototypes of these two land cover classes are spectrally very similar, and as the merging criterion of the single linkage method is exclusively based on minimum distance they are erroneously grouped into a single cluster. Since the merging criterion utilized by the proposed method uses more information about the data in addition to inter-cluster distances, it does not allow that prototypes of the sandy soil and area urban classes be merged at the initial levels. Although the spatial boundary index of these two classes has presented a low value (given that the spatial boundary between them is considerable), the CDbw and spatial compactness indices presented relatively high values, preventing thus an early fusion of the two classes.

Continuing with the application of the proposed classification methodology, the modified version of the CDbw cluster validation index was applied at all of the levels of the dendrogram to determine which cluster configuration of the 52 that were obtained is ideal. Fig. 6 shows the validation index values in the modified and the original form. The graph only shows the values between levels 38 and 51 of the dendrogram. For levels lower than 38 the index values are smaller than those on the graph, or even null, due to the existence of levels composed of clusters with a single prototype. The number of clusters or classes from level 38 to 51 decreases from 15 to 2, respectively.

As expected, the strategy of modifying the cluster validation index computation has approximation errors, but the variation of their values occurs in a similar way to the original

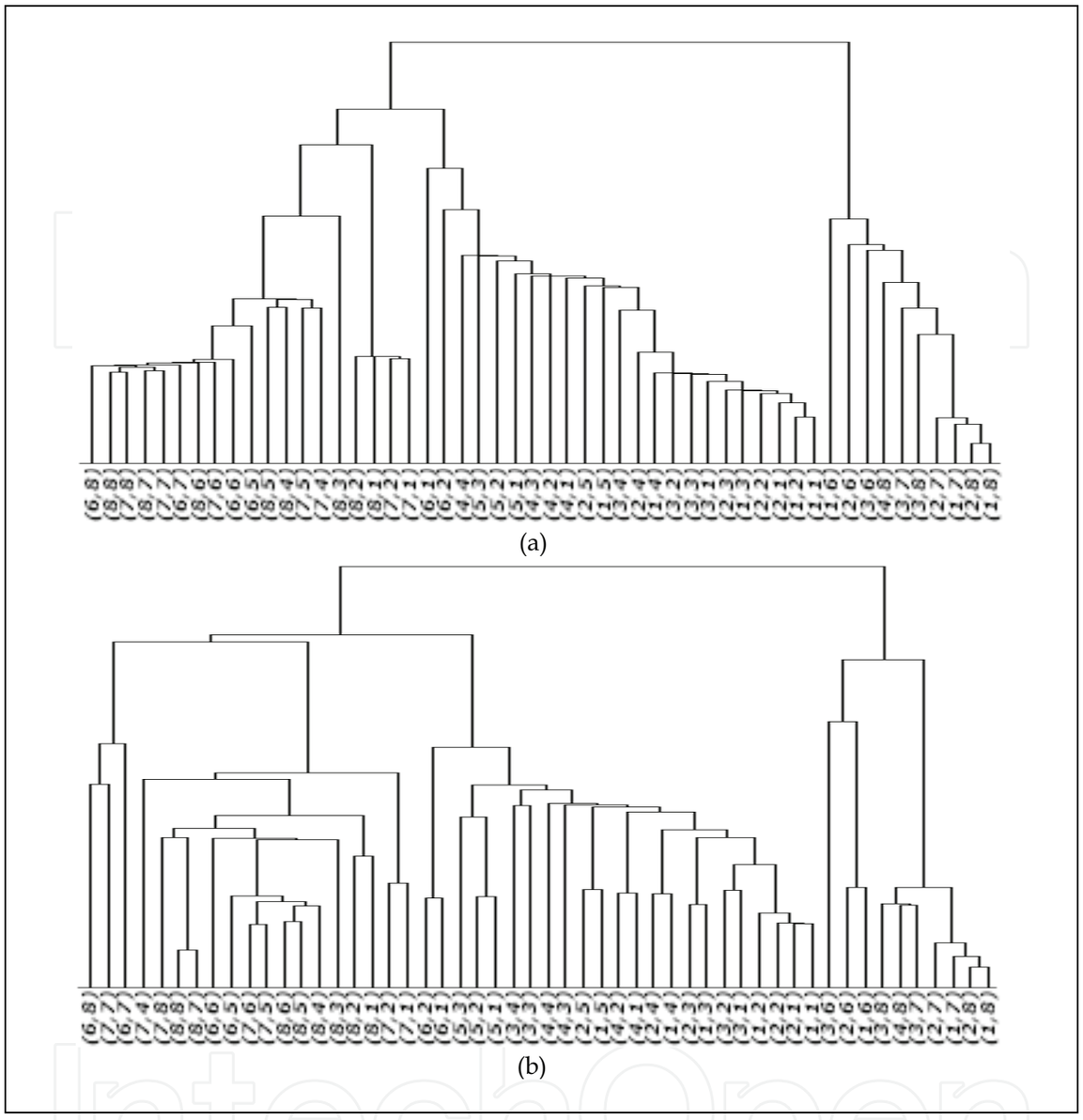

Fig. 5. Dendrograms of the SOM prototypes using different merging criteria. (a) Proposed merging criterion. (b) Single linkage method using only spectral information. The ordered pairs correspond to the positions of the SOM prototypes in the 8×8 grid.

version, not compromising the decision making process regarding the ideal number of data clusters. The main advantage of using the modified version of the index is its processing time. In this experiment, while the time to calculate the CDbw index in the original form (for the entire dendrogram) was 478 seconds, the modified version needed only 26 seconds. It is important to note that this significant difference occurs due to the volume of data considered for each of the ways to calculate the index. Calculation of the CDbw index in its original form was executed at each level of the dendrogram considering the 1521 samples collected in the image, while the modified version calculation considered only 64 SOM prototypes and their respective activity levels.

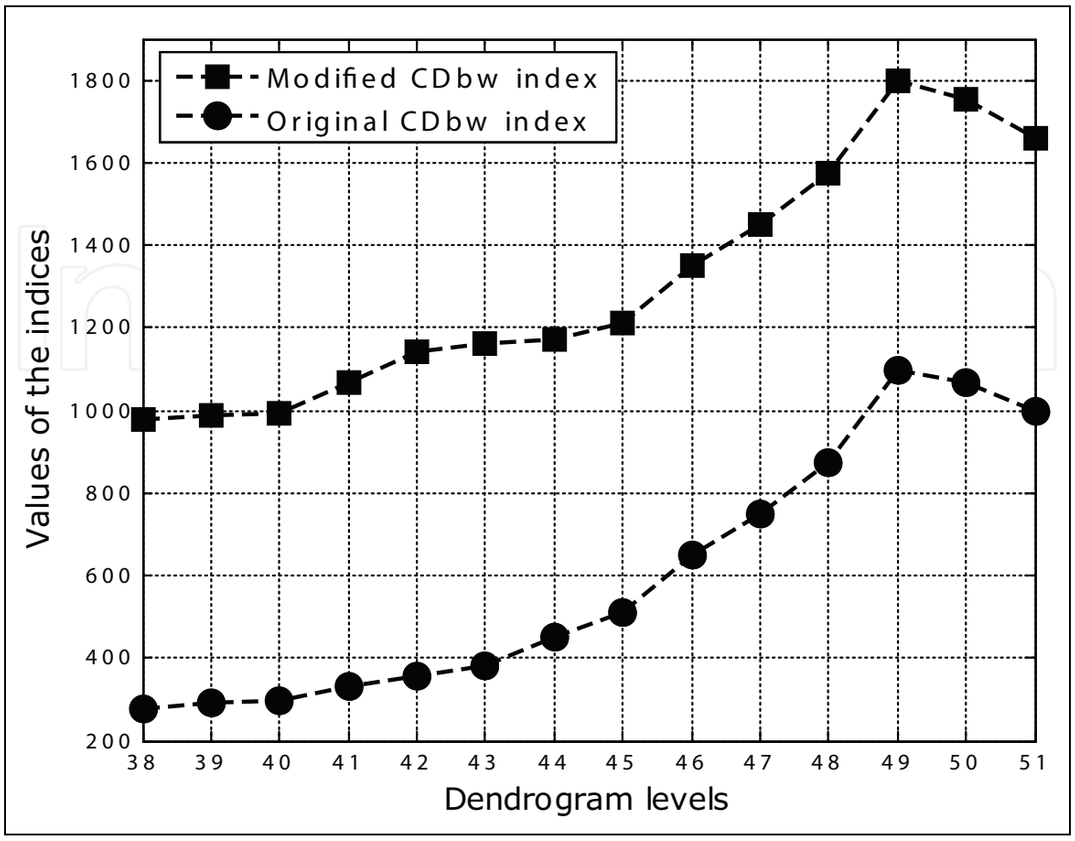

Fig. 6. CDbw index values in the modified and the original form

For the CDbw index, the greater its value, the better the result. Considering this, of all of the dendrogram levels obtained in this experiment, level 49 is the one that has the greatest value for the index (as can be seen in Fig. 6), and thus, the best cluster configuration for the SOM prototypes. Fig. 4b shows the SOM grid image classified in accordance with the clusters (classes) of level 49. Compared to the SOM grid image in Fig. 4a, it can be seen that the SOM prototypes are grouped into 4 classes, adequately corresponding to the 4 large land cover classes present in the image (water, sandy soil, vegetation, and urban area). The squares marked with "o" and "×" are, respectively, the inactive and heterogeneous prototypes that were discarded in the filtering process of the proposed method. It is interesting to see that these prototypes act as "interpolation units" and certainly contribute to the class separation process.

To finish, the original image was classified comparing 7×7 pixel windows with all of the labeled SOM prototypes (except the inactive prototypes). According to the proposed method, a total of 7643 pixels associated with the heterogeneous prototype class were reclassified using the neighboring pixel class that had the least (spectral) distance. Fig. 7a shows the classification result of test image 1 using the proposed methodology (the 4 classes are represented with the same colors used in Fig. 4b).

Fig. 7b shows the result of the image classification by the *K*-means algorithm considering the number of classes as being equal to 4. The algorithm was executed using five different initializations for the centroids of each of the classes and a maximum number of iterations equal to 100.

Unlike the proposed method, the *K*-means algorithm did not discriminate the sandy soil pattern in the image and classified the vegetation areas in two categories. The sandy soil pattern is only differentiated by the *K*-means algorithm if the number of clusters (*k*) is set to greater or equal to 7. Moreover, performing a visual analysis of the classification results obtained by the two methods it is possible to verify that the image classified by proposed methodology has a superior visual aspect. While the classification of the image by the *K*-means algorithm appears more dotted, the image produced by the proposed method is more homogenous in all of the classified areas. The difference in appearance is certainly due to the way the two methods extract the information from the image. While the *K*-means algorithm applied here uses a pixel-by-pixel approach, the proposed method works with pixel windows which incorporate the neighborhood information of pixels. In both classification results some vegetation areas were erroneously classified as water pattern due to topographic shadowing effects.

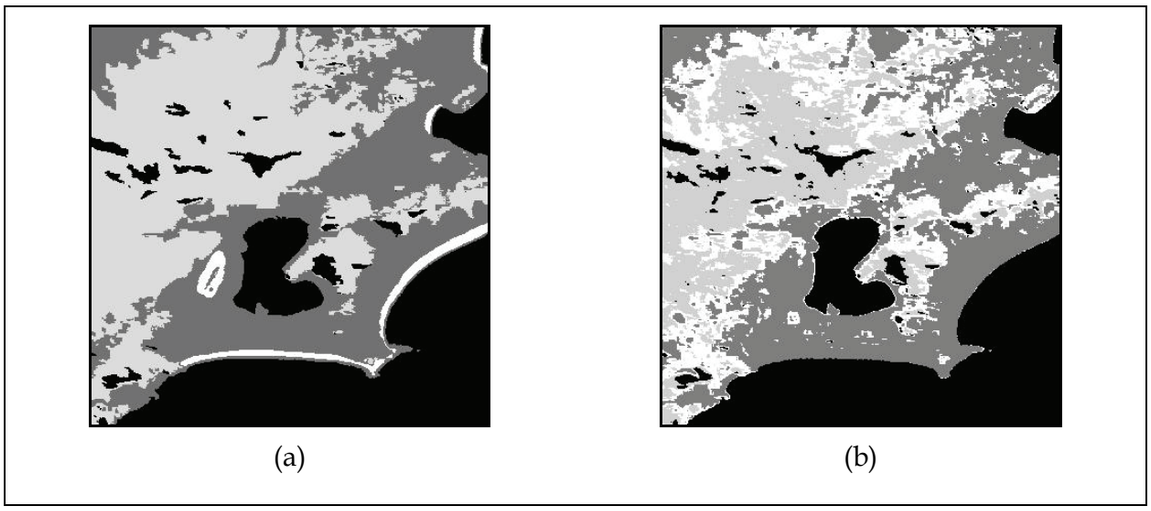

(a) (b)

Fig. 7. (a) Test image 1 classified by the proposed method. (b) Test image 1 classified by the K-means algorithm considering k=4.

Attempting to perform a less subjective analysis of the image classified by the proposed method, and considering the absence of terrestrial truth for the test image, the present work performed the classification of the test image in a supervised manner and considers these results as a reference (or "true"). The supervised classification, considering the 4 predominant classes in the image, was done by means of a multilayers *Perceptrons* neural net. This class of neural nets has been widely employed to perform supervised classification of remotely sensed images (Özkan & Erbek, 2003).

The Kappa agreement index was calculated by comparison of the image classified by the proposed method and the reference image (resulting from the supervised classification). Considering that the Kappa index reached the value of 0.89, we can consider that the classification result of the test image 1 by method presented in this work was satisfactory.

4.2 Experiment 2

The second experiment was performed on a segment taken from an IKONOS image. It has an IFOV of 4 m and is composed of three bands in the visible spectrum. The segment used in

this experiment has 350 lines and 384 columns. This imagery shows irrigation pivots in the region of Andaraí in the state of Bahia, Brazil, and presents six land cover classes: sparse vegetation, forest, two types of bare soil, and two types of growing crop. Fig. 8 shows the segment of the original image (denominated here as test image 2).

Following the procedures of the proposed method, 1292 sample windows of size 9×9 were collected from test image 2 and used to train a SOM composed of 144 neurons arranged in a 12×12 rectangular grid. Fig. 9a shows the SOM grid image after training in which it is possible to visualize prototype clusters that correspond to the land cover classes present in the original image. As in experiment 1, topological ordering and density matching properties of the mapping produced by the SOM can be seen. Land cover classes with similar spectral attributes are mapped to neighboring regions of the two-dimensional output grid and those that occupy larger areas in the original image are mapped to a larger number of prototypes of the grid.

Fig. 8. Color composite of the test image 2 (provided by Engesat/Brazil, © Space Imaging)

After the SOM training, the prototype filtering process was applied. In this experiment 15 SOM prototypes presented null activity, and 14 presented a high degree of spectral heterogeneity. Thus, of the 144 total prototypes, 29 of them were filtered, leaving 115 SOM prototypes to be analyzed.

In sequence, the agglomerative hierarchical method was applied on the filtered SOM prototypes. A dendrogram consisting of 115 levels was generated, each level with a different configuration of SOM prototype clusters. The modified version of the CDbw index was applied at all of the levels of the dendrogram to determine which of the 115 cluster configurations that were obtained was ideal. Level 110 had the greatest value for the validation index, and therefore, the best cluster configuration for the SOM prototypes. Fig. 9b shows the SOM grid image classified in accordance with the clusters (classes) of level 110. Compared to the SOM grid image in Fig. 9a, it can be seen that the SOM prototypes are grouped into 6 classes, adequately corresponding to the 6 land cover classes present in the original image.

As in experiment 1, it is important to point out that the correct segmentation of the SOM grid is only reached due to the merging criterion employed by the proposed method. If only the inter-cluster distances were used to decide about the cluster fusion, certainly different

prototype classes would be erroneously grouped into a single cluster in the SOM grid. For example, the SOM prototypes corresponding to forest and growing crop 1 classes are spectrally very similar. As can be viewed in the SOM grid image (Fig. 9a), they are close to one another in the upper left corner of the grid. These two prototype classes are correctly discriminated by the proposed method because the indices used in the merging criterion (especially the spatial boundary and spatial compactness indices) presented high values, preventing thus an early fusion of the two classes. In fact, as can be seen in the original image (Fig. 8), the areas corresponding to forest and growing crop 1 classes (situated respectively in the lower left corner and in the upper right corner of the image) do not have common boundary and are spatially compact. It is fundamental to note also that the adequate segmentation of the SOM is facilitated by the prototype filtering process applied on it. The inactive and heterogeneous prototypes that were discarded in the filtering process act as "borders" in the SOM grid contributing considerably to the separation of the clusters.

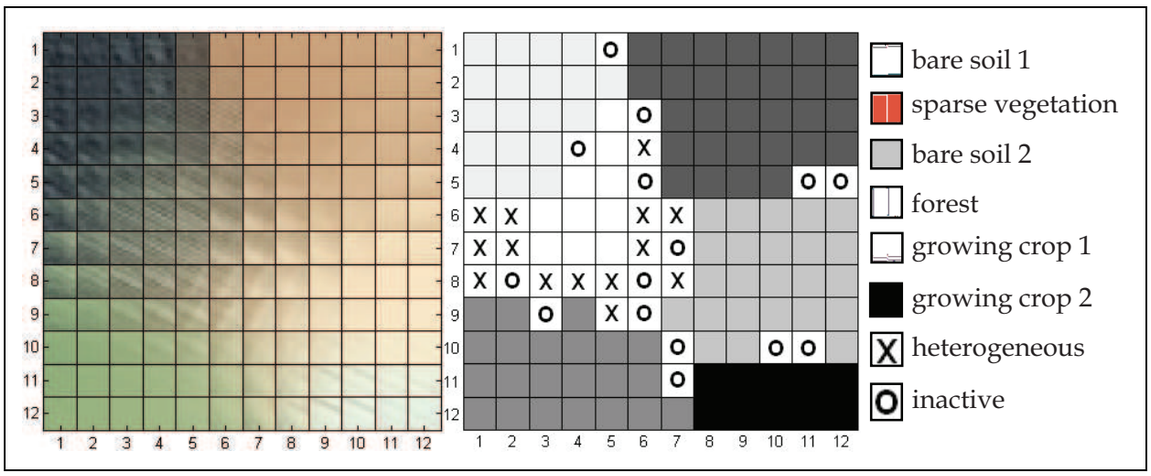

Fig. 9. (a) SOM grid image obtained from test image 2. (b) Classified SOM grid.

Fig. 10a shows the classification result of test image 2 using all of the labeled SOM prototypes, except the inactive prototypes (the 6 classes are represented with the same colors used in Fig. 9b). A total of 19717 pixels associated with the heterogeneous prototypes were reclassified using the neighboring pixel class that had the least (spectral) distance. Fig. 10b shows the result of the classification of the same image by K-means algorithm setting the number of classes at 6.

Performing a visual analysis of the results obtained by the two methods it is possible to clearly verify a large difference between the two classifications. The proposed method adequately classified the different land cover patterns present in the original image without any significant confusion between them. On the other hand, the K-means algorithm did not correctly discriminate the patterns and presented a relatively erroneous classification. It did not differentiate the growing crop 2 class (in the lower right corner of the image) from one of the bare soil patterns, and it also confused the forest class with the growing crop 1 class. Just as in the classification results of experiment 1, the classification of the test image 2 by the K-means algorithm were more speckled, while the image produced by the proposed method is considerably more homogeneous in all of the classified areas. This difference in appearance is more accentuated in this experiment because test image 2 presents a higher spatial resolution than test image 1. In test image 2, the land cover classes have more well defined

textural features, and because the proposed method uses the neighborhood information of the pixels, it produces a superior result to the K-means algorithm, which uses a pixel-by-pixel approach.

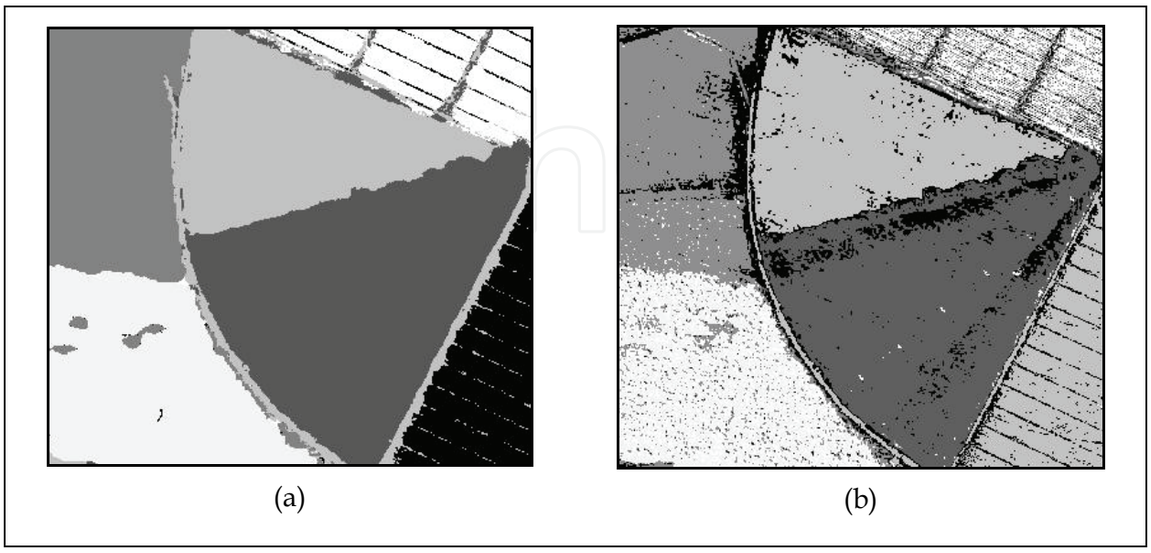

Fig. 10. (a) Test image 2 classified by the proposed method. (b) Test image 2 classified by the K-means algorithm considering k=6.

Although the quality of the classification produced by the proposed method is visually superior, the image used in this experiment also was classified in a supervised manner and the result of this classification was used as a reference to evaluate the results obtained by the two methods. As in experiment 1, the supervised classification was done by means of a multilayers Perceptrons neural net. The Kappa index was then calculated individually for the images produced by the proposed method and by the K-means algorithm. Confirming the visual impression of the results, the image classified by the K-means algorithm had a Kappa value of 0.74, while the image classified by the proposed method had a value equal to 0.92.

4.3 Processing time

Table 1 shows the processing times spent in the two experiments by the main stages of the proposed classification methodology. All of the experiments presented here were performed with MATLAB software and a microcomputer with an AMD Athlon™ 2600+ 1,91GHZ processor and 1 GB of RAM. The global time consumed to perform the classifications of test images 1 and 2 were, respectively, 143 and 236 seconds.

A comparison between the processing times consumed by proposed methodology and the K-means algorithm to classify the test images is not appropriate here. As previously mentioned, the two methods have principles and characteristics that are very different, which should be considered in the evaluation of its calculation complexities.

An important difference between the methods is in the quantity of classes they analyze in order to classify the image. The proposed method evaluates different cluster configurations for the data, whereas the K-means algorithm performs the classification of the scene only for a single quantity of classes defined a priori. In the experiment 1, for example, the time spent by the proposed method to evaluate 52 different cluster

configurations was 26 seconds, using SOM prototypes to represent the image data and the CDbw validation index with modified calculation. If we were to use a similar strategy to the K-means algorithm, i.e., perform different classifications of the image varying the number of classes (k) and then apply the CDbw validation index to determine which was better, the processing time would be so high that the strategy would be considered impracticable. It is enough to take into consideration the time spent in applying the CDbw index to evaluate the classification produced by the K-means algorithm shown in Fig. 7b. It took 979 seconds, far more than the time spent by the proposed method to evaluate diverse cluster configurations for the image. Even though the CDbw validation index has a good level of computational complexity in comparison to others, the high number of points in remotely sensed images generates a very high processing volume to execute its calculations.

Taking these observations into account and also considering the possible benefits of the techniques and procedures employed in the methodology proposed, we can conclude that the processing time consumed by the method presented here is perfectly admissible, certifying its application viability.

Stages	Consumed time (in seconds)	
	Experiment 1	Experiment 2
Sampling	8	7
SOM training	34	56
Prototypes filtering	2	4
Agglomerative hierarchical analysis	29	96
Clusters evaluation	26	42
Image classification	44	31
Total	143	236

Table 1. Processing time consumed by the proposed method

5. Conclusions and final considerations

In this work, an unsupervised method of classifying remotely sensed images based on clustering of the SOM was presented. The key point of the proposed method is to perform the cluster analysis of the image through a set of SOM prototypes instead of working directly with the original patterns of the scene.

The proposed methodology presents benefits and potentialities that make it as a differentiated alternative to perform the unsupervised classification of remotely sensed images. Among these, we can point out:

1. The two-level clustering approach based on SOM significantly reduces the computational load of the classification process, making it possible to use methods that have not normally been considered computationally viable for the processing of

remotely sensed images, such as hierarchical clustering methods and cluster validation indices.

2. Another benefit in executing the clusters analysis of the image through a set of SOM prototypes is noise reduction. The SOM prototypes are local averages of the data, and therefore less sensitive to random variations than the original data of the image.
3. The method does not require a previous definition of the number of classes to perform the classification of the image. It does not occur in the majority of the conventional unsupervised classification methods, such as K-means.
4. The distributed representation of the classes by means of prototype groups gives the method the potential to discover geometrically complex and varied data clusters. Methods such as K-means use a single prototype (centroid) to represent each class and because of this are only capable of adequately detecting clusters that have spherical formats.
5. The simple use of pixel windows allows contextual information to be included without any explicit calculation of measure for it. This approach contributes to the quality of the resulting classification.
6. The proposed method has only two parameters that must be defined by the user (the size of the samples and the number of SOM neurons), and despite this it is very robust as far as these choices. Conventional methods (such as K-means and ISODATA) are very sensitive to a quantity of user-dependent parameters.
7. The utilization of an agglomerative hierarchical clustering method for clustering the SOM allows the user to observe the relationships that exist between the land cover patterns existing in the image at different cluster levels. It can be very helpful in applications where the structure of the information present in the image is not clearly known.
8. The proposed method employs an efficient merge mechanism that incorporates more information about the data in each cluster. Traditional clustering methods use only inter-cluster distance information to decide about the merging of clusters.
9. The method can determine, without any user intervention, the ideal number of clusters or classes for the image.

In addition to the test image utilized in the experiments shown here, the proposed method has also been applied to other high and medium resolution images, with satisfactory results. However, it is important to observe that the performance of the proposed method highly depends on the quality of the SOM mapping. The use of the procedures and techniques presented here assumes that the SOM has been successfully trained. In this way, questions about topological distortions and density approximation produced by the mapping of the net can be better investigated. Moreover, SOM variants were not used in this work because we wanted to select the most frequently used version of SOM. Therefore, new SOM developments could naturally be applied to further increase the potential of the proposed classification methodology.

6. References

Azcarraga, A. P., (2000) Assessing self-organization using order metrics, Proceedings of IEEE-INNS-ENNS International Joint Conference on Neural Networks, July, Como, Italy, 6:159-164.

Ball, G., and Hall, D., (1967) A clustering technique for summarizing multivariate data, Behavior Science, 12:153-155.

Bandyopadhyay, S., (2005) Satellite image classification using genetically guided fuzzy clustering with spatial information, International Journal of Remote Sensing, 26(3): 579-593.

Costa, J. A. F., and Netto, M. L. A. (1999) Estimating the Number of Clusters in Multivariate Data by Self-Organizing Maps. Intl. Journal of Neural Systems, vol. 9, pp. 195-202.

Costa, J. A. F., and Netto, M. L. A. (2001) Clustering of complex shaped data sets via Kohonen maps and mathematical morphology". In: Proceedings of the SPIE, Data Mining and Knowledge Discovery. B. Dasarathy (Ed.), Vol. 4384, pp. 16-27.

Duda, T., and Canty, M., (2002) Unsupervised classification of satellite imagery: choosing a good algorithm, International Journal of Remote Sensing, 23(11): 2193-2212.

Gonçalves, M. L., Andrade Netto, M. L., Costa, J. A. F., Zullo Jr., J., (2005) Automatic Remotely Sensed Data Clustering by Tree-Structured Self-Organizing Maps, Proceedings of IEEE International Geoscience and Remote Sensing (IGARSS'05), 25-29 July, Seoul, Korea, 4 p.

Gonçalves, M. L., Andrade Netto, M. L., Costa, J. A. F., Zullo Jr., J., (2006) Data Clustering using Self-Organizing Maps segmented by Mathematic Morphology and Simplified Cluster Validity Indexes: an application in remotely sensed images, Proceedings of IEEE International Joint Conference on Neural Networks, July, Vancouver, p. 8854-8861.

Hadjimitsis, D.G, Evangelou I., Lazakidou A., and Clayton C.R.I., (2003) Unsupervised Classification of Remotely Sensed Images Using Self-Organizing Maps for mapping land-cover changes, Proceedings of the Remote Sensing and Photogrammetry Society Annual Conference, September, Nottingham, UK, 7 p.

Halkidi, M., and Vazirgiannis, M., (2002) Clustering validity assessment using multi representatives, Proceedings of SETN Conference, April, Thessaloniki, Greece.

Haralick, R. M., Shanmugam, K., and Dinstein, I., (1973) Textural features for image classification, IEEE Transactions on Systems, Man and Cybernetics, 3(6): 610-621.

Huang, K., (2002) The use of a newly developed algorithm of divisive hierarchical clustering for remote sensing image analysis, International Journal of Remote Sensing, 23(16):3149-3168.

Ji, C. Y., (2000) Land-use classification of remotely sensed data using Kohonen self-organizing feature map neural networks, Photogrammetric Engineering and Remote Sensing, 66(12):1451-1460.

Ji, M., (2003) Using fuzzy sets to improve cluster labeling in unsupervised classification, International Journal of Remote Sensing, 24(4):657–671.

Kelly, M., Shaari, D., Guo, Q, and Liu, D., (2004) A comparison of standard and hybrid classifier methods for mapping hardwood mortality in areas affected by

"sudden oak death", Photogrammetric Engineering and Remote Sensing, 70(11):1229-1239.

Kohonen, T., (1997) Self-Organizing Maps, 2nd Ed., Berlim: Springer Verlag.

Liu, A., Bi-Cheng, L., Chen, G., and Zhangiu, X, (2005) A new ART neural networks for remote sensing image classification, Lecture Notes in Computer Science, 3611:37-42.

Magnussen, S., Boudewyn, P., and Wulder, M., (2004) Contextual classification of Landsat TM images to forest inventory cover types, International Journal of Remote Sensing, 25(12):2421-2440.

Marçal, A. R. S., and Borges, J. S., (2005) Estimation of the "natural" number of classes of a multispectral image. Proceedings of IEEE International Geoscience and Remote Sensing Symposium (IGARSS'05), 25-29 July, Seoul, Korea, 6: 3788-3791.

Marçal, A. R. S., and Castro, L., (2005) Hierarchical clustering of multispectral images using combined spectral and spatial criteria, IEEE Geoscience and Remote Sensing Letters, 2(1):59-63.

Merkl, D., and Rauber, A., (1997) Alternative ways for cluster visualization in self-organizing maps. Proceedings of the Workshop on Self-organizing Maps (WSOM97), June, Finland, 106-111.

Özkan, C., and Erbek, F. S., (2003) A Comparison of activation functions for multispectral Landsat TM image classification, Photogrammetric Engineering and Remote Sensing, 69(11):1225-1234.

Sezgin, M., Ersoy, O. K. and Yazgan, B., (2004) Segmentation of remote sensing images using multistage unsupervised learning. Proceedings of SPIE, Applications of Digital Image Processing XXVII, August, Colorado, USA, 5558:616-623.

Shah, C. A., Arora, M. K., and Varshney, P. K., (2004) Unsupervised classification of hyperspectral data: an ICA misture model based approach, International Journal of Remote Sensing, 25(2):481-487.

Tran, T. N., Wehrens, R., and Buydens, L. M. C., (2003) Sparef: a clustering algorithm for multiespectral images, Analytica Chimica Acta, 490(1):303-312.

Tran, T. N., Wehrens, R., and Buydens, L. M. C., (2005) Clustering multispectral images: a tutorial, Chemometrics and Intelligent Laboratory Systems, 77(1-2):3-17.

Tso, B, and Olsen, R. C., (2005) Combining spectral and spatial information into hidden Markov models for unsupervised image classification, International Journal of Remote Sensing, 26(10):2113-2133.

Vesanto, J., and Alhoniemi, E., (2000) Clustering of the Self-organizing Map. IEEE Transactions on Neural Networks, 11(3):586-602.

Vilmann, T., Merenyi, E., and Hammer, B., (2003) Neural maps in remote sensing image analysis, Neural Networks, 16(3):389-403.

Wang, J., Delabie, J., Aasheim, H. C., Smeland, E., and Myklebost, O., (2002) Clustering of the SOM easily reveals distinct gene expression patterns: results of a reanalysis of lymphoma study, BMC Bioinformatics, 3:36.

Wilson, H. G., Boots, B., and Millward, A. A., (2002) A comparison of hierarchical and partitional clustering techniques for multispectral image classification, Proceedings

of IEEE International Geoscience and Remote Sensing Symposium (IGARSS'02), 24-28 June, Toronto, Canada, (3):1624-1626.

Wu, S., and Chow, T. W. S., (2004) Clustering of the Self-organizing Map using a clustering validity index based on inter-cluster and intra-cluster density, Pattern Recognition, 37:175-188.

Xu, R., and Wunsch II, D., (2005) Survey of clustering algorithms, IEEE Transactions on Neural Networks, 16(3):645-678.

IntechOpen

IntechOpen

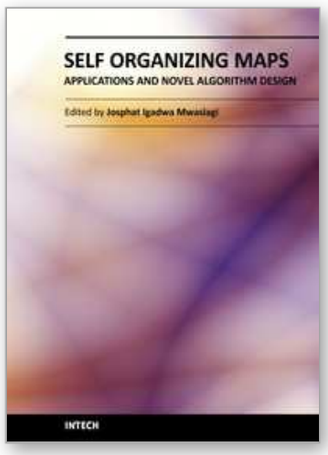

Self Organizing Maps - Applications and Novel Algorithm Design
Edited by Dr Josphat Igadwa Mwasiagi

ISBN 978-953-307-546-4
Hard cover, 702 pages
Publisher InTech
Published online 21, January, 2011
Published in print edition January, 2011

Kohonen Self Organizing Maps (SOM) has found application in practical all fields, especially those which tend to handle high dimensional data. SOM can be used for the clustering of genes in the medical field, the study of multi-media and web based contents and in the transportation industry, just to name a few. Apart from the aforementioned areas this book also covers the study of complex data found in meteorological and remotely sensed images acquired using satellite sensing. Data management and envelopment analysis has also been covered. The application of SOM in mechanical and manufacturing engineering forms another important area of this book. The final section of this book, addresses the design and application of novel variants of SOM algorithms.

How to reference
In order to correctly reference this scholarly work, feel free to copy and paste the following:

M. L. Gonçalves, J. A. F. Costa and M. L. A. Netto (2011). Land-Cover Classification Using Self-Organizing Maps Clustered with Spectral and Spatial Information, Self Organizing Maps - Applications and Novel Algorithm Design, Dr Josphat Igadwa Mwasiagi (Ed.), ISBN: 978-953-307-546-4, InTech, Available from: http://www.intechopen.com/books/self-organizing-maps-applications-and-novel-algorithm-design/land-cover-classification-using-self-organizing-maps-clustered-with-spectral-and-spatial-information

INTECH
open science | open minds

InTech Europe
University Campus STeP Ri
Slavka Krautzeka 83/A
51000 Rijeka, Croatia
Phone: +385 (51) 770 447
Fax: +385 (51) 686 166
www.intechopen.com

InTech China
Unit 405, Office Block, Hotel Equatorial Shanghai
No.65, Yan An Road (West), Shanghai, 200040, China
中国上海市延安西路65号上海国际贵都大饭店办公楼405单元
Phone: +86-21-62489820
Fax: +86-21-62489821

© 2011 The Author(s). Licensee IntechOpen. This chapter is distributed under the terms of the Creative Commons Attribution-NonCommercial-ShareAlike-3.0 License, which permits use, distribution and reproduction for non-commercial purposes, provided the original is properly cited and derivative works building on this content are distributed under the same license.

IntechOpen

IntechOpen